

Collisional-Radiative Modeling of W^{27+*}

Xiaobin DING, Izumi MURAKAMI, Daiji KATO, Hiroyuki A. SAKAUE, Fumihiro KOIKE¹⁾
and Chenzhong DONG²⁾

National Institute for Fusion Science, 322-6 Oroshi-cho, Toki 509-5292, Japan

¹⁾*School of Medicine, Kitasato University, Sagami-hara, Kanagawa 252-0373, Japan*

²⁾*College of Physics and Electronic Engineering, Northwest Normal University, Lanzhou 730070, China*

(Received 9 December 2011 / Accepted 10 July 2012)

A detailed collisional radiative model of W^{27+} ions was constructed based on the atomic data calculated by relativistic atomic properties software Flexible Atomic Code. The strong electric dipole (E1) transitions mainly comes from the $4f \rightarrow 4d$ transition in W^{27+} ions with wavelength falls into VUV region (4.6 - 5.1 nm), while the wavelength of magnetic dipole (M1) transition among the fine structures of the first excited states falls into the visible optical region. Synthetic spectra in both regions are given theoretically with plasma condition in EBIT for experiment reference. Finally, the dependence of the intensity ratio on the electron density is provided as a potential diagnostic tool of Maxwellian plasmas.

© 2012 The Japan Society of Plasma Science and Nuclear Fusion Research

Keywords: tungsten, plasma diagnosis, collisional radiative modeling

DOI: 10.1585/pfr.7.2403128

1. Introduction

Tungsten (W) attracts research interest because it is one of the good candidates for the divertor or wall material in the next generation magnetic confinement fusion reactors due to its favorable properties. These applications have motivated a number of theoretical and experimental investigations on the atoms (ions) radiative properties over a rather large temperature range [1–10]. Tungsten impurity ions might be transported to the core plasma and radiate high energy photons. Consequently, large radiation loss could be caused by these impurity ions. However, tungsten impurities can also provide information about fusion plasmas such as electron density, electron temperature and ion temperature.

In the last three decades, extensive research has been done on the radiative properties of highly charged W ions. Measurements of radiation from tungsten ions have been carried out at many Electron Beam Ion Trap (EBIT) ion sources and fusion devices. A review of the research work on the tungsten ions which had been done before 2008 is given in [1]. Ralchenko *et al.* measured the M1 transitions of $3d^n$ configuration of highly-charged tungsten ions. The spectrum were analyzed by a hybrid collisional-radiative modeling [11]. They also suggested several M1 line ratios which could be used to reliably diagnose the temperature and density in hot plasma. For high temperature plasma, Yanagibayashi *et al.* observed EUV spectra of highly charged W ions from JT-60U plasma at $T_e \approx 8$ and 14 keV [12, 13]. For low temperature plasma, Ab-

dallah *et al.* construct a collisional radiative modeling of tungsten for $T_e = 1 - 2$ eV [14]. We also measured the visible spectrum of moderate ionized W^{26+} ions using the EBIT facility, and the spectrum were analyzed via multi-configuration Dirac-Fock calculations [15, 16].

In the ASDEX Upgrade, the Ni-like W^{46+} to Kr-like W^{38+} ions were expected to be observed in the central plasma region and Rb-like W^{37+} to Sn-like W^{24+} ions were expected in the outer plasma region [6]. It can be expected that the W^{26+} and W^{27+} ions will be abundant in the outer region of ITER as in ASDEX Upgrade. For the impurity control and plasma diagnostics, it is necessary to have thorough knowledge about these ions.

The ground state of W^{27+} is $4d^{10}4f^1$ which has only one electron in the open $4f$ orbital. This ion can be chosen as the first example to be investigated due to its relative simplicity. Other lower-charge ions in which the ground state has more than two electrons in the open $4f$ orbital will lead to more complicated situation for detailed fine structure collisional radiative (CR) modeling.

The paper is organized as follows. Section 2 describes the CR modeling method and the procedure to obtain the necessary atomic data. The VUV and optical spectrum as well as potential diagnosis lines are discussed in Sec 3. Finally, the last section summaries the conclusion.

2. Theoretical Method

The emission intensity (I_{ij}) of a specific transition from upper energy level i to lower energy level j of an atom in the plasma is proportional to the product of the radiative decay rate (A_{ij}) and population density (n_i) of the upper level i , i.e.,

author's e-mail: ding.xiaobin@LHD.nifs.ac.jp

^{*)} This article is based on the presentation at the 21st International Toki Conference (ITC21).

$$I_{ij} \propto n_i A_{ij}. \quad (1)$$

With the development of atomic theory based on relativistic quantum dynamics and modern computer technology, the radiative transition rate A_{ij} can be determined accurately by state-of-the-art theoretical calculations. The relativistic configuration interaction method as implemented in the Flexible Atomic Code (FAC) [17] was used to calculate the atomic data which are necessary to construct the CR model. Relativistic effects and the important electron correlation effects have been taken into account.

The state population density n_i can be obtained by solving the collisional-radiative rate equation:

$$\begin{aligned} \frac{dn_i}{dt} = & \sum_{j<i} C(j, i) n_e n_j \\ & - \left\{ \left[\sum_{j<i} F(i, j) + \sum_{j>i} C(i, j) + S(i) \right] n_e \right. \\ & \left. + \sum_{j<i} A(i, j) \right\} n_i \\ & + \sum_{j>i} [F(j, i) n_e + A(j, i)] n_j, \end{aligned} \quad (2)$$

where n_e is the electron density, $C(j, i)$ and $F(j, i)$ are collisional excitation and deexcitation rates from the level j to i , $A(j, i)$ is the radiative transition rate from the level j to i , $S(i)$ is the collisional ionization rate of the level i of W^{27+} ions to W^{28+} ions. The radiative transition, collisional (de) excitation and ionization processes are included in the present calculation, while the radiative and dielectronic as well as three body recombination processes are not included because these processes only slightly affect the population of the low-lying levels that are relevant to the present spectrum.

The fine-structure levels of the configurations $4d^{10}4f$, $4d^{10}5l$, $4d^{10}6l$, $4d^9 4f^2$, $4d^9 4f^1 5l$ ($l \leq 4$) of W^{27+} were included in the present calculation. The rates of radiative transitions and the collisional-(de)excitation among these levels were calculated using the relativistic configuration interaction method. All the possible E1, E2, E3, and M1, M2 transition among these fine-structure levels are calculated. The collisional excitation cross section was calculated in the distorted wave approximation. The collisional ionization processes from the levels of W^{27+} ions mentioned above to the levels of configuration $4d^{10}$, $4d^9 4f$, $4d^9 5l$, $4d^8 4f^2$ and $4d^8 4f 5l$ of W^{28+} are included.

Experimentally, the atomic properties of these ions can be measured accurately by the electron beam ion trap (EBIT) facilities. With the CR modeling, the experimental measurement can be analyzed reliably. This method was successfully used in many previous studies to analyze and identify dozens of spectral lines from highly charged heavy ions in x-ray and VUV as well as optical regions.

To simulate the emission spectrum in EBIT and fusion plasma, the free electron are assumed to be mono-energy

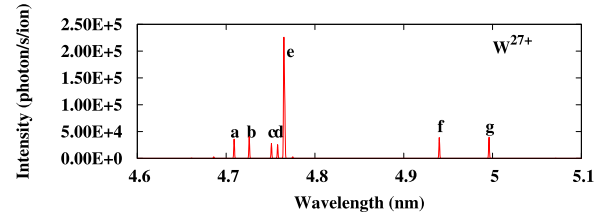


Fig. 1 The synthetic spectrum of W^{27+} ions in 4.6-5.1 nm with $n_e = 10^{10} \text{ cm}^{-3}$ and $E_e = 830 \text{ eV}$, the electron distribution were assumed to be in mono-energy like in EBIT.

Table 1 The wavelength (λ in nm) and transition probability (A_{ij} in 10^{12} s^{-1}) of W^{27+} ions in VUV region. The upper and lower levels denoted by the open relativistic orbital and its occupation number as well as total angular momentum J in subscript. The column ‘‘Key’’ present the corresponding label in Fig. 1.

λ (nm)	$A_{ij}(10^{12} \text{ s}^{-1})$	Upper levels	Lower Levels	Key
4.709	6.58	$[4d_{3/2}^3 4f_{5/2}^2]_{5/2}$	$[4f_{5/2}]_{5/2}$	a
4.726	7.01	$[4d_{3/2}^3 4f_{5/2} 4f_{7/2}]_{7/2}$	$[4f_{7/2}]_{7/2}$	b
4.751	6.06	$[4d_{3/2}^3 4f_{5/2} 4f_{7/2}]_{5/2}$	$[4f_{7/2}]_{7/2}$	c
4.758	6.53	$[4d_{3/2}^3 4f_{5/2}^2]_{3/2}$	$[4f_{5/2}]_{5/2}$	d
4.765	6.81	$[4d_{3/2}^3 4f_{5/2} 5s_{1/2}]_{3/2}$	$[5s_{1/2}]_{1/2}$	e
4.766	6.79	$[4d_{3/2}^3 4f_{5/2} 5s_{1/2}]_{1/2}$	$[5s_{1/2}]_{1/2}$	e
4.940	4.24	$[4d_{3/2}^3 4f_{5/2} 4f_{7/2}]_{9/2}$	$[4f_{7/2}]_{7/2}$	f
4.996	4.04	$[4d_{3/2}^3 4f_{5/2}^2]_{7/2}$	$[4f_{5/2}]_{5/2}$	g

and Maxwellian, respectively, during the calculation of the rate coefficients. The individual transition lines were assumed to have Gaussian profile with FWHM = 0.01 nm for VUV region and 0.1 nm for visible region, respectively, which can take the instrument and the thermal Doppler broadening effects into account.

3. Results and Discussions

Identification of the strong transitions is the basic step of both atomic physics and plasma diagnosis. The synthetic spectrum of W^{27+} ions in 4.6-5.1 nm is shown in Fig. 1. The electron distribution was assumed to be mono-energetic (with $E_e = 830 \text{ eV}$) that results can be used to compare with a future EBIT experiment. All the strong emission lines of W^{27+} ions in this wavelength region come from the electric dipole (E1) transition $4f \rightarrow 4d$. The transition e comes from $4d^9 4f 5s \rightarrow 4d^{10} 5s$, while others come from the resonance transition $4d^9 4f^2 \rightarrow 4d^{10} 4f$. The corresponding transition wavelengths and transition probabilities are listed in Table 1.

Forbidden transitions in highly charged ions become prominent in low density plasma because the population densities of the excited levels which decay only via forbidden transitions can be relatively high and therefore produce some strong radiation. The synthetic spectrum of W^{27+} ions in the visible region (340-750 nm) was given in Fig. 2 with the same plasma condition as in VUV case. The

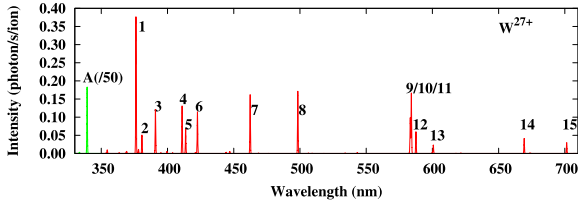


Fig. 2 The synthetic spectrum of W^{27+} ions in optical region with $n_e = 10^{10} \text{ cm}^{-3}$ and $E_e = 830 \text{ eV}$, the electron distribution were assumed to be in mono-energy like in EBIT. The intensity of peak A was divided by 50 to fit the display.

Table 2 The wavelength (λ in nm) and transition probability (A_{ij} in s^{-1}) of W^{27+} ions in visible region. The upper and lower levels denoted by the open relativistic orbital and its occupation number as well as total angular momentum J in subscript. The column “Key” present the corresponding label in Fig. 2.

$\lambda(\text{nm})$	$A_{ij}(\text{s}^{-1})$	Upper levels	Lower Leves	Key
339.3	295.00	$[4d^{10}4f_{7/2}]_{7/2}$	$[4d^{10}4f_{5/2}]_{5/2}$	A
376.2	156.80	$[(4d_{5/2}^5 4f_{5/2})_2 4f_{7/2}]_{11/2}$	$[(4d_{5/2}^5 4f_{5/2})_1 4f_{7/2}]_{9/2}$	1
380.7	80.63	$[4d_{5/2}^5 4f_{7/2}^2]_{11/2}$	$[(4d_{5/2}^5 4f_{5/2})_5 4f_{7/2}]_{11/2}$	2
390.9	62.07	$[(4d_{5/2}^5 4f_{5/2})_5 4f_{7/2}]_{13/2}$	$[(4d_{5/2}^5 4f_{5/2})_2 4f_{7/2}]_{11/2}$	3
411.0	134.20	$[(4d_{5/2}^5 4f_{5/2})_5 4f_{7/2}]_{11/2}$	$[(4d_{5/2}^5 4f_{5/2})_2 4f_{7/2}]_{11/2}$	4
413.7	70.31	$[4d_{5/2}^5 4f_{7/2}^2]_{11/2}$	$[(4d_{5/2}^5 4f_{5/2})_5 4f_{7/2}]_{9/2}$	5
422.6	47.62	$[(4d_{5/2}^5 4f_{5/2})_2 4f_{7/2}]_{11/2}$	$[4d_{5/2}^5 4f_{5/2}^2]_{13/2}$	6
462.4	170.10	$[4d_{5/2}^5 4f_{7/2}^2]_{11/2}$	$[(4d_{5/2}^5 4f_{5/2})_3 4f_{7/2}]_{13/2}$	7
498.4	51.62	$[4d_{5/2}^5 4f_{7/2}^2]_{11/2}$	$[(4d_{5/2}^5 4f_{5/2})_1 4f_{7/2}]_{13/2}$	8
582.8	3.89	$[(4d_{5/2}^5 4f_{5/2})_5 4f_{7/2}]_{11/2}$	$[(4d_{5/2}^5 4f_{5/2})_3 4f_{7/2}]_{13/2}$	9
583.3	29.58	$[4d_{5/2}^5 4f_{7/2}^2]_{11/2}$	$[4d_{5/2}^5 4f_{5/2}^2]_{13/2}$	10
584.1	84.68	$[4d_{5/2}^5 4f_{7/2}^2]_{15/2}$	$[(4d_{5/2}^5 4f_{5/2})_5 4f_{7/2}]_{13/2}$	11
587.6	12.96	$[(4d_{5/2}^5 4f_{5/2})_3 4f_{7/2}]_{11/2}$	$[(4d_{5/2}^5 4f_{5/2})_5 4f_{7/2}]_{15/2}$	12
600.7	9.62	$[(4d_{5/2}^5 4f_{5/2})_2 4f_{7/2}]_{11/2}$	$[4d_{5/2}^5 4f_{5/2}^2]_{9/2}$	13
669.3	24.04	$[4d_{5/2}^5 4f_{5/2}^2]_{13/2}$	$[(4d_{5/2}^5 4f_{5/2})_5 4f_{7/2}]_{11/2}$	14
701.4	34.40	$[(4d_{5/2}^5 4f_{5/2})_4 4f_{7/2}]_{13/2}$	$[(4d_{5/2}^5 4f_{5/2})_4 4f_{7/2}]_{11/2}$	15

strong magnetic dipole (M1) transitions of W^{27+} ions may fall into the visible region. The strongest transition (peak A in Fig. 2) with wavelength 339.3 nm in the present calculation (343.4 nm in detailed multi-configuration Dirac-Fock calculation [18]) is the M1 transition between the doublet of the ground state $4d^{10}4f^2 F_{7/2}$ and $^2F_{5/2}$. A new observation in Toyko-EBIT (344.40 nm) might corresponding to this peak [19]. The difference between the present calculation result and detailed MCDF calculation mainly due to the different treatment on the complex electron correlation effects. Generally, MCDF method can deal with electron correlation effects better. Both method has an accuracy about 1% on the transition wavelength. The wavelength of M1 transitions among the fine structure of first excited configuration $4d^9 4f^2$ also falls into the visible spectrum region, but the intensity is weaker than that of peak A. The corresponding transition wavelengths and transition prob-

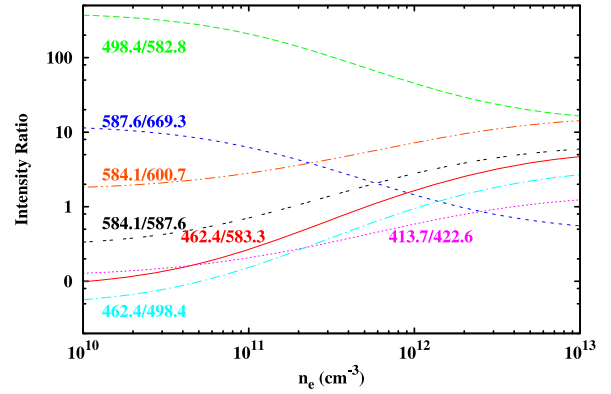


Fig. 3 Electron density dependence of the intensity ratio in optical region in EBIT environment ($E_e = 830 \text{ eV}$ with electron distribution were assumed to be mono-energy).

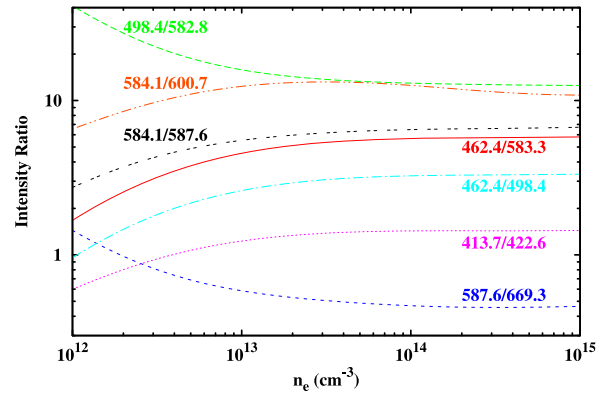


Fig. 4 Electron density dependence of the emission line intensity in optical region with $T_e = 1 \text{ KeV}$, the electron distribution were assumed to be Maxwellian like in fusion plasma.

abilities as well as designation are listed in Table 2.

The intensities (number of photon per second per ion) in Fig. 2 is much weaker than that of Fig. 1 by 6 orders. This means the most favorable transition is E1 resonance transition from the first excited state. The visible spectrum can only be observed within the appropriate plasma conditions in which the excited state have larger population.

The diagnostic potential of the transition lines for the electron density is based on the electron density dependence of the selected line intensity ratios. When collisional rates become comparable with the radiative transition probabilities of a specific level, the intensity ratio shows sensitivity to the electron density n_e .

The electron density dependence of the intensity ratios in optical region for EBIT environment are given in Fig. 3 for some selected transition lines of diagnostics interests. The figure shows that these intensity ratios are sensitive to the electron density from 10^{10} cm^{-3} to 10^{13} cm^{-3} . The results are expected to be verified in the further EBIT experiment measurements.

Finally, for the fusion plasma diagnostics purpose, the free electron distribution was assumed to be Maxwellian with electron temperature $T_e = 1$ KeV. The potential diagnostics lines in visible optical region are shown in Fig. 4. All the selected optical lines are density-sensitive in the low density region for fusion plasma.

4. Conclusion

A detailed CR model for W^{27+} ions was constructed and theoretical synthetic spectra were provided in the present paper. Electric dipole transition $4f \rightarrow 4d$ dominate in the VUV region, and magnetic dipole transition of the first excited states $4d^9 4f^2$ of W^{27+} fall into the visible region. Several transitions are predicted to be sensitive to the electron density and can be used for diagnostics. Further experimental measurements are desired. However, for the optical visible spectrum measurements in EBIT, the most important is to find an effective way to generate the excited ions with abundant population. Because M1 transition generally have small transition probability, the experiment measurement may need relatively longer exposure time.

Acknowledgement

The author would like to thank Dr. N. Nakamura and Prof. R. More for the valuable discussion and suggestion. The referee's considerate comments and advice for revising the manuscript are appreciated. This work was performed partly as one of the subjects of IAEA's Co-ordinated Research Project (CRP) in 'Spectroscopic and Collisional Data for Tungsten from 1 eV to 20 keV' and partly with the support and under the auspices of the JSPS Grant-in-Aid for Scientific Research(A) 23246165. One of the authors (Xiaobin Ding) would like to express his thanks

to NIFS for giving him the opportunity to work as a COE faculty.

- [1] J. Reader, Phys. Scr. **T134**, 014023 (2009).
- [2] R. Radtke, C. Biedermann, J.L. Schwob *et al.*, Phys. Rev. A **64**, 012720 (2001).
- [3] R. Radtke, C. Biedermann, P. Mandelbaum *et al.*, J. Phys.: Conf. Ser. **58**, 113 (2007).
- [4] C. Biedermann and R. Radtke, AIP Conf. Proc. **1161**, 95 (2009).
- [5] C. Biedermann, R. Radtke, R. Seidel *et al.*, J. Phys.: Conf. Ser. **163**, 012034 (2009).
- [6] C. Biedermann, R. Radtke, R. Seidel *et al.*, Phys. Scr. **T134**, 014026 (2009).
- [7] T. Nakano, N. Asakura, H. Kubo *et al.* Nucl. Fusion **49**, 115024 (2009).
- [8] J. Clementson, P. Beiersdorfer, G.V. Brown *et al.*, Phys. Scr. **81**, 015301 (2010).
- [9] J. Clementson, P. Beiersdorfer, E.W. Magee *et al.*, J. Phys. B: At. Mol. Opt. Phys. **43**, 144009 (2010).
- [10] C.S. Harte, C. Suzuki, T. Kato *et al.*, J. Phys. B: At. Mol. Opt. Phys. **43**, 205004 (2010).
- [11] Y. Ralchenko, I.N. Draganić, D. Osin *et al.*, Phys. Rev. A **83**, 032517 (2011).
- [12] J. Yanagibayashi, T. Nakano, A. Iwamae *et al.*, J. Phys. B: At. Mol. Opt. Phys. **43**, 144013 (2010).
- [13] J. Yanagibayashi, T. Nakano, A. Iwamae *et al.*, Nucl. Instrum. Methods A **623**, 741 (2010).
- [14] J. Abdallah Jr, J. Colgan, R.E.H. Clark *et al.*, J. Phys. B: At. Mol. Opt. Phys. **44**, 075701 (2011).
- [15] A. Komatsu, J. Sakoda, N. Nakamura *et al.*, Phys. Scr. **2011**, 014012 (2011).
- [16] X.B. Ding, F. Koike, I. Murakami *et al.*, J. Phys. B: At. Mol. Opt. Phys. **44**, 145004 (2011).
- [17] M.F. Gu, Can. J. Phys. **86**, 675 (2008).
- [18] X.B. Ding, F. Koike, I. Murakami *et al.*, J. Phys. B: At. Mol. Opt. Phys. **45**, 035003 (2012).
- [19] H. Watanabe, N. Nakamura, D. Kato *et al.*, Can. J. Phys. **90**, 497 (2012).